



UNIVERSITI TEKNIKAL MALAYSIA MELAKA

**FINITE ELEMENT ANALYSIS OF TYRE USING EULERIAN
APPROACH**

This report submitted in accordance with requirement of the Universiti Teknikal
Malaysia Melaka (UTeM) for the Bachelor Degree of Mechanical Engineering
(Automotive) with Honours.

By


KONG LEARN FEI

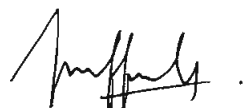
FACULTY OF MECHANICAL ENGINEERING

2011

SUPERVISORS DECLARATION


“I hereby, declare that I have read this report and in my opinion, this report is sufficient in terms of scope and quality for the award of the degree of Bachelor of Mechanical Engineering (Automotive)”

Signature : 
1st Supervisor's Name : DR. MUHAMMAD ZAHIR HASSAN
Date : 16 MAY 2011

Signature : 
2nd Supervisor's Name : DR. NOREFFENDY BIN TAMALDIN
Date : 16 MAY 2011

DECLARATION

I hereby, declared this report entitled “Finite Element Analysis of Tire Using Eulerian Approach” is the results of my own research except as cited in references.

Signature : 
Student's Name : KONG LEARN FEI
Date : 16 MAY 2011

ABSTRACT

Automotive pneumatic tyre plays an important role for vehicle suspension system. Development process of tyre involved experiments which are time consuming and expensive, hence increase the tyre development cost. In order to overcome this problem, many other methods have been implemented. One of these methods is Finite Element Analysis. This aims of this project are to develop a simplified 185/70 R14 pneumatic tyre model to study road/ tyre interaction using Finite Element Method by using ABAQUS software. This project started with 2D axisymmetric tyre modeling to perform rim mounting and inflation analysis followed by 3D tyre model by revolving the 2D mesh developed. The footprint and steady state rolling analysis are performed to study the behavior of tyre when in contact with the road surface during loaded and rolling condition where this analysis is very complicated that involved high experiment cost. Instead of carry out experiment, the computational method is used to study the tyre behavior. Real tyre components are considered in this project which included one carcass, two belts and rubber matrix. In axisymmetric model, element group of CGAX3H and CGAX4H from ABAQUS are used to define the element for rubber matrix and the tyre reinforcement are represented as rebar in surface elements, SFGAX1 are embedded into the continuum elements. After the analysis of tyre using CAE, the results are validated with result from previous research.

ABSTRAK

Tayar pneumatik Otomotif memainkan peranan yang penting dalam suspensi kenderaan. Proses pembangunan tayar melibatkan percubaan eksperimen yang memakan masa dan mahal, lalu meningkatkan kos pembangunan tayar. Untuk mengatasi masalah ini, banyak kaedah lain telah dilaksanakan dan dicuba. Salah satu daripada kaedah tersebut adalah Analisis Elemen Hingga. Tujuan projek ini adalah untuk menyediakan model tayar 185/70 R14 yang diringkaskan untuk mengkaji interaksi tayar dengan permukaan jalan dengan Kaedah Elemen Hingga menggunakan software ABAQUS. Projek ini dimula dengan membentuk model asimetrik 2D untuk melakukan mounting dan analisis inflasi dan akhirnya model 3D tayar dibentuk dengan memutar mesh daripada mesh model 2D. Analisis tapak permukaan tayar and analisi putaran tayar dalam keadaan mantap dilakukan untuk mempelajari perilaku permukaan jalan dengan tayar di mana tayar dalam keadaan dimuat, diisi dengan angin and analisi putaran tayar atas permukaan jalan sangat rumit dan melibatkan kos eksperimen yang tinggi. Dari menggunakan kaedah eksperimen, kaedah analisi menggunakan komputer digunakan untuk mengkaji perilaku tayar. Sifat komponen tayar yang sebenar digunakan dalam projek ini. Ia termasuklah salah satu carcass, dua steel belts dan getah matriks. Dalam model axisimetrik, elemen kumpulan CGAX3H dan CGAX4H dari ABAQUS digunakan untuk mendefinisikan unsur untuk getah matriks dan penguat tayar yang merupakan sebagai Rebar pada unsur permukaan, SFMGAX1 di mana akan tertanam ke dalam elemen kontinum. Setelah analisis ban menggunakan CAE, hasil analisis dibukti dengan percubaan eksperimen yang dimudahkan.

DEDICATION

This report is dedicate for my beloved family who never failed to give me financial and moral support, for giving all my need during the time I developed my system and for teaching me that even the largest task can be accomplished if it is done one step at a time.

I also want to send this message to my soul mate who always give moral support during hard time.

TABLE OF CONTENTS

| | |
|------------------------------------|----------|
| SUPERVISORS DECLARATION | i |
| DECLARATION | ii |
| ABSTRACT | iii |
| ABSTRAK | iv |
| DEDICATION | v |
| ACKNOWLEDGEMENT | vi |
| TABLE OF CONTENTS | vii |
| LIST OF TABLES | xv |
| LIST OF FIGURES | xvii |
| LIST OF ABBREVIATIONS | xxiv |
| | |
| 1. CHAPTER 1: INTRODUCTION | 1 |
| 1.1 Overview | 1 |
| 1.2 Problem Statements | 2 |
| 1.3 Objectives | 2 |
| 1.4 Scope and Limitations of Study | 3 |
| 1.5 Organization of Thesis | 4 |

| | | |
|-----------|--|----------|
| 2. | CHAPTER 2: LITERATURE REVIEW | 5 |
| 2.1 | Tire | 7 |
| 2.2 | History of Tire | 7 |
| 2.3 | Tire components | 9 |
| 2.4 | Tire Designation | 11 |
| 2.5 | Tire Classification | 13 |
| 2.5.1 | Radial Ply Tire | 13 |
| 2.5.2 | Non Radial Ply Tire | 14 |
| 2.5.3 | Differences in the dynamics of radial and non-radial tires | 14 |
| 2.6 | Theory Research | 15 |
| 2.6.1 | Non Linear Finite Element Analysis | 15 |
| 2.6.2 | Arbitrary Lagrangian-Eulerian | 16 |
| 2.6.2.1 | Lagrangian Method | 16 |
| 2.6.2.2 | Eulerian Method | 17 |
| 2.6.3 | Characterization of material constants based on synthetic biaxial data | 19 |
| 2.7 | Application and Field of Tire Finite Elements Analyses | 20 |
| 2.8 | Tire Model | 22 |
| 2.9 | Tire Rubber Matrix | 24 |
| 2.10 | Reinforcement | 27 |
| 2.11 | 2D Tire Model Discretization | 27 |
| 2.12 | 3D Tire Modeling | 28 |
| 2.13 | Rim | 29 |
| 2.14 | Loading Steps and Analyses | 27 |
| 2.14.1 | Load Deflection Validation | 31 |
| 2.15 | Steady State Free Rolling Of Tire | 32 |

| | | |
|-----------|---|-----------|
| 2.16 | Tyre Modal Analysis | 36 |
| 2.17 | Summary | 37 |
| 3. | CHAPTER 3: METHODOLOGY | 39 |
| 3.1 | Introduction of Theory and Tire Finite Elements | 39 |
| 3.2 | Geometry of the 2 Dimensional Tire | 42 |
| 3.3 | Tire Components Material | 45 |
| 3.3.1 | Rubber properties | 45 |
| 3.3.2 | Reinforcement Material | 47 |
| 3.4 | Element for 2 Dimensional Tire Model | 50 |
| 3.4.1 | Rim contact and tread area meshing element | 50 |
| 3.4.2 | Boundary Conditions | 51 |
| 3.4.2.1 | Rim | 51 |
| 3.4.2.2 | Symmetric Point | 51 |
| 3.4.3 | Constraints | 51 |
| 3.4.3.1 | Embedded Elements | 51 |
| 3.4.4 | Axisymmetric Rim Mounting and Inflation | 52 |
| 3.4.4.1 | Rim Constraints | 52 |
| 3.4.4.2 | Loading Step | 52 |
| 3.4.4.3 | Inflation Analysis | 52 |
| 3.4.4.4 | Field of Interest for 2 D Inflation Analyses - Field Output request | 53 |
| 3.5 | Axisymmetric 2 D Full Tire Model | 53 |
| 3.6.1 | 3D Modelling for Footprint Analyses | 56 |
| 3.6.1.0 | Geometry of Present Study Tyre Model (185/70R14) | 57 |
| 3.6.1.1 | Symmetric Result Transfer and Symmetric Geometrical Transfer | 59 |

| | | |
|-----------|---|-----------|
| 3.6.1.2 | Boundary Conditions | 59 |
| 3.6.1.3 | Boundary Condition for Step 0 of the Simulation | 60 |
| 3.6.1.4 | Boundary Condition for Step 1 of the Simulation | 62 |
| 3.6.1.5 | Boundary Condition for Step 2 of the Simulation | 62 |
| 3.6.1.6 | Boundary Condition for Step 3 of the Simulation | 62 |
| 3.6.1.7 | Loading Steps | 62 |
| 3.6.1.8 | Symmetric Result Transfer And Symmetric Geometrical Transfer | 63 |
| 3.7 | Steady State Rolling Analyses | 65 |
| 3.7.1 | Steady-State Rolling Analysis, Full Braking and Traction Analysis | 65 |
| 3.7.2 | Steady-State Rolling Analysis, Braking Analysis | 67 |
| 3.7.3 | Steady State Rolling Analyses, Traction Analysis | 67 |
| 4. | CHAPTER 4: 2D TYRE INFLATION AND RIM MOUNTING ANALYSES | 69 |
| 4.1 | 2D Tyre inflation and Rim Mounting Analyses | 69 |
| 4.1.1 | Inflation Analysis and Bead Fitment | 69 |
| 4.1.2 | Assumption Made | 70 |
| 4.1.3 | Rim Mounting Process | 70 |
| 4.2 | Two Dimensional Axisymmetric Half Tyre Model Inflation Analysis | 71 |
| 4.2.1 | Stress Result of Finite Element Analysis | 71 |
| 4.2.2 | Deformed Magnitude through Finite Element Analysis | 72 |
| 4.2.3 | Deformed Direction Through Finite Element Analysis | 72 |
| 4.3 | Two Dimensional Axisymmetric Full Tyre Model Inflation Analyses | 76 |
| 4.3.1 | Stress Result of Finite Element Analyses (Full 2D Tyre Model) | 76 |

| | | |
|-----------|---|-----------|
| 4.3.2 | Deformed Magnitude through Finite Elements Analyses | 77 |
| 4.3.3 | Deformed Direction through Finite Elements Analyses (2D Axisymmetric Full Tyre Model) | 80 |
| 4.3.4 | Computational Cost for Half 2D Axisymmetric Tyre Model Analyses | 80 |
| 4.4 | Discussion | 81 |
| 5. | CHAPTER 5: FREE-FREE MODAL ANALYSIS | 84 |
| 5.1 | Introduction | 84 |
| 5.2 | Finite Element Analysis of Tyre Free-free Modal | 85 |
| 5.2.1 | FEA Solution Strategy | 86 |
| 5.3 | Result of Finite Element Analysis (1,0) mode | 87 |
| 5.4 | Summary | 89 |
| 6. | CHAPTER 6: PARTIAL 3D TYRE FOOTPRINT ANALYSIS | 90 |
| 6.1 | Partial 3D tyre footprint analysis | 90 |
| 6.1.1 | Introduction | 90 |
| 6.2 | Partial 3D Tyre Model Description | 91 |
| 6.2.1 | Meshing | 91 |
| 6.2.2 | Boundary Condition | 91 |
| 6.3 | Assumption for Partial 3D Footprint Analysis | 92 |
| 6.4 | Deformation of partial 3D tyre after footprint analysis with load of 1650N | 93 |
| 6.5 | Stress Distribution of Partial 3D Tyre After Footprint Analysis With Load of 1650N | 95 |
| 6.5.1 | Stress Distribution of Tyre Steel Belt Member 1 | 95 |

| | | |
|-----------|--|------------|
| 6.5.2 | Stress Distribution of Tyre Steel Belt Member 2 | 95 |
| 6.5.3 | Stress Distribution of Tyre Carcass | 96 |
| 6.5.4 | Stress Distribution of Tyre Rubber Matrix | 97 |
| 6.6 | Shear Stress Distribution in Plane | 98 |
| 6.7 | Footprint Contact Path Analysis | 99 |
| 6.7.1 | Consideration in Contact Path Analysis in ABAQUS | 100 |
| 6.8 | Elements Type and Number of Elements in Partial 3D Tyre Footprint Analysis | 101 |
| 6.9 | Summary of Result of Partial 3D Tyre Footprint Analysis | 102 |
| 6.10 | Comparison Of Present Research Model with Koishi, et.al 1998 Model | 103 |
| 7. | CHAPTER 7: FULL 3D TYRE FOOTPRINT ANALYSIS | 105 |
| 7.1 | Full 3D Tyre Footprint Analysis | 105 |
| 7.1.1 | Introduction | 105 |
| 7.2 | Partial 3D Tyre Model Description | 105 |
| 7.2.1 | Model Meshing | 105 |
| 7.2.2 | Boundary Conditions | 106 |
| 7.3 | Assumption for Full 3D Footprint Analysis | 106 |
| 7.4 | Deformation of Full 3D Tyre Footprint analysis | 107 |
| 7.5 | Stress Distribution of Full 3D Tyre Footprint Analysis | 109 |
| 7.5.1 | Stress Distribution of Steel Belt Member 1 | 109 |
| 7.5.2 | Stress Distribution of Steel Belt Member 2 | 110 |
| 7.5.3 | Stress Distribution of Tyre Carcass | 110 |
| 7.6 | Discussion | 111 |
| 7.7 | Full 3D Tyre Model Footprint Contact Path Analysis | 111 |

| | | |
|-----------|---|------------|
| 7.8 | Comparison of Result from Partial 3D Tyre and Full 3D Tyre Modal Footprint Analysis | 113 |
| 7.9 | Elements Type and Number of Elements in Full 3D Tyre Footprint Analysis | 114 |
| 7.10 | Summary of Result of Full 3D Tyre Footprint Analysis | 114 |
| 8. | CHAPTER 8: STEADY- STATE ROLLING ANALYSIS | 116 |
| 8.1 | Steady-State Rolling Analysis | 116 |
| 8.1.1 | Introduction | 116 |
| 8.2 | 3D Tyre Modal Description | 117 |
| 8.2.1 | Meshing | 117 |
| 8.3 | Boundary Conditions | 117 |
| 8.3.1 | Straight Line Rolling, Full Braking Condition | 117 |
| 8.4 | Assumptions Made | 118 |
| 8.5 | Full 3D Tyre Contact Pressure of Steady –state Rolling Analysis | 118 |
| 8.5.1 | Tyre Contact Pressure of Steady State Rolling Analysis with Time, Full Braking | 118 |
| 8.5.2 | Tyre Contact Pressure of steady state rolling analysis with time, full traction | 119 |
| 8.6 | Full 3D Tyre Contact Shear Stress of Steady –State Rolling Analysis | 120 |
| 8.6.1 | Tyre Contact Shear Stress of Steady State Rolling Analysis, Full Braking | 120 |
| 8.6.2 | Tyre Contact Shear Stress of Steady State Rolling Analysis, Full Traction | 121 |
| 8.7 | Full 3D Tyre Deformation of Steady –State Rolling Analysis | 123 |
| 8.7.1 | Tyre deformation at Steady State Rolling Analysis, Full braking | 123 |

| | | |
|-----------|--|------------|
| 8.7.2 | Tyre deformation at Steady State Rolling Analysis, Full Traction | 125 |
| 8.8 | Stress Distribution in Tyre Reinforced Members | 127 |
| 8.8.1 | Stress in Tyre Belt Member during Braking | 127 |
| 8.8.2 | Stress Distribution in Tyre Belt Member 1 during Traction Step with Time | 127 |
| 8.8.3 | Stress Distribution in Tyre Belt Member 2 during Braking | 129 |
| 8.8.4 | Stress Distribution in Tyre Belt Member 2 during Traction Step with Time | 129 |
| 8.8.5 | Stress Distribution in Tyre Carcass Rolling Analysis | 131 |
| 9. | CHAPTER 9: CONCLUSION AND RECOMMENDATION | 132 |
| 9.1 | Conclusion | 132 |
| 9.2 | Recommendation | 135 |
| | REFERENCES | 136 |
| | APPENDIX I | 141 |
| | APPENDIX II | 143 |
| | APPENDIX III | 144 |

LIST OF TABLES

| | | |
|-----------|---|-----|
| Table 2.9 | Material information for Mooney-Rivlin rubber model | 26 |
| Table3.1 | Tyre rubber matrix properties | 45 |
| Table3.2 | Density | 45 |
| Table3.3 | Material Properties for Mooney-Rivlin material model | 46 |
| Table3.4 | Material Properties for Polynomial, N=1 material model | 46 |
| Table3.5 | Density | 46 |
| Table3.6 | Marlow, Uniaxial Test Data | 46 |
| Table3.7 | Carcass material information | 47 |
| Table3.8 | Rebar layer | 48 |
| Table3.9 | Belt material Information | 48 |
| Table3.10 | Rebar layer | 48 |
| Table4.1 | Comparison of stress analyses for 2D tyre model analyses | 82 |
| Table4.2 | Comparison of deformed magnitude for 2D tyre model analyses | 82 |
| Table4.3 | Comparison of computational cost for 2D tyre model analyses | 83 |
| Table5.1 | Material properties of tyre model for free-free modal analysis | 86 |
| Table5.2 | Meshing of the full 3D tyre model for the finite element free-free modal analysis | 87 |
| Table6.8 | Number of Element and Element Type in Partial 3D Tyre Footprint Analysis | 101 |

| | | |
|-----------|--|-----|
| Table6.9 | Maximum Von Mises Stress in Tyre Components | 102 |
| Table6.10 | Maximum Deformation in Tyre Components | 102 |
| Table6.11 | Tyre contact path after loading of 1650N | 102 |
| Table6.12 | Comparison of simulation results from Koishi, et.al. 1998 model with present research model | 103 |
| Table7.7 | Comparison of simulation results of partial 3D tyre footprint analysis and full 3D tyre footprint analysis | 113 |
| Table7.9 | Number of Element and Element Type in Full 3D Tyre Footprint Analysis | 114 |
| Table7.10 | Maximum Von Mises Stress in Tyre Components | 114 |
| Table7.11 | Maximum Deformation in Tyre Components | 115 |
| Table7.12 | Tyre contact path after loading of 1650N | 115 |
| Table8.1 | Tyre contact shear stress distribution during steady state rolling analysis, full braking condition | 121 |
| Table8.2 | Summarized result full 3D tyre Contact Shear Stress during full traction step with time. | 122 |
| Table8.3 | Summary of longitudinal deformation of tyre footprint area during full braking step | 124 |
| Table8.4 | Summary of longitudinal deformation of tyre footprint area during full traction step | 126 |

LIST OF FIGURES

| | | |
|------------|---|----|
| Figure 2.1 | Flow Chart of Literature Review | 6 |
| Figure2.3 | Components of radial tires (Gent (2007)) | 9 |
| Figure2.4 | Tire designation | 11 |
| Figure2.5 | Cross section of a tire on a rim with tire height and width | 12 |
| Figure2.6 | Construction of radial tire | 13 |
| Figure2.7 | Example of non-radial tire interior | 14 |
| Figure2.8 | Ground sticking behaviour of radial and non-radial tires in the presence of a lateral force. | 14 |
| Figure 2.9 | The creation of FE model based on curves and surfaces exported from CAD model | 23 |
| Figure2.10 | CAD Tread pattern modeling technique | 24 |
| Figure2.11 | Specimens and additional equipment used to obtain material data for purely rubber structural components of tires. | 26 |
| Figure2.12 | 3D tire model for vertical loading analysis | 30 |
| Figure2.13 | Dial gauges arrangement for measure deflection | 31 |
| Figure2.14 | The correlation between longitudinal force and angular speed | 33 |
| Figure2.15 | Determination of angular velocity at free rolling by fine increment around initial value, obtained from straight line rolling analysis. | 33 |

| | | |
|------------|---|----|
| Figure2.16 | Oscillograph image of single point of tyre. (Image from Pottinger, M.G, 2006) | 34 |
| Figure2.17 | Normal stress isometric for a radial medium duty (TBR) truck tire rolling at zero slip and inclination angle. (Tyre Science and Technology, vol.27, No.3, 1999 with Tyre Society) | 35 |
| Figure2.18 | Deformation of tyre during static and rolling condition (Tire Science and Technology, Vol.20, No.1, 1992) | 35 |
| Figure3.1 | Flow for the tire finite element analyses. | 40 |
| Figure3.2 | Flow chart of finite element analysis of present research | 41 |
| Figure3.3 | The two dimensional tire modeling by using axisymmetric approach | 42 |
| Figure3.4 | The steps for the 2 dimensional tire modeling | 43 |
| Figure3.5 | 2D reinforce modeling technique | 44 |
| Figure3.6 | Orientation of carcass and $\pm 20^{\circ}$ of belts | 48 |
| Figure3.7 | Orientation of Steel Belt Member 1 of Present Research Model | 49 |
| Figure3.8 | Orientation of Steel Belt Member 1 of Present Research Model | 49 |
| Figure3.9 | The sharp edges of the tire profile are discretized with triangular hybrid element with twist. | 50 |
| Figure3.10 | The other areas of the tire are discretized with tetrahedral hybrid elements that give lower computational cost compared to quadrilateral element. | 50 |

| | | |
|-------------|---|----|
| Figure3.11 | The symmetric point of the half 2 dimensional tires are discard after the tire geometry is reflected using mirror option in ABAQUS. | 51 |
| Figure3.12 | The carcass and the belt are embedded into the rubber matrix of tire | 52 |
| Figure3.12a | The algorithm of 2 dimensional full tire inflation analyses | 54 |
| Figure3.13 | 2D axisymmetric half tire model is reflected using mirror option in ABAQUS/ CAE | 55 |
| Figure3.14 | The process of performing 3 dimensional footprint analyses | 56 |
| Figure3.15 | Geometrical Dimension of present study tyre | 57 |
| Figure3.16 | Element control for partial 3D tyre modelling | 58 |
| Figure3.17 | Node sets created for anti-symmetry boundary conditions, ASYMA and ASYMC | 60 |
| Figure3.18 | Node sets created for anti-symmetry boundary conditions, ASYMA | 60 |
| Figure3.19 | Node sets created for anti-symmetry boundary conditions, ASYMC | 60 |
| Figure3.20 | Node sets created for anti-symmetry boundary conditions, ASYMB and ASYMD | 61 |
| Figure3.21 | Node sets created for anti-symmetry boundary conditions, ASYMB | 61 |
| Figure3.22 | Node sets created for anti-symmetry boundary conditions, ASYMD | 61 |
| Figure3.23 | Node sets created and defined as SYM | 62 |
| Figure3.24 | Node sets created and defined as SYM1 | 62 |

| | | |
|-------------|---|----|
| Figure3.25 | Equation of defining anti-symmetry boundary condition | 62 |
| Figure 3.26 | Key coding of the SMG and SRT in ABAQUS | 64 |
| Figure 3.27 | Flow of the Steady-State Rolling Analysis | 66 |
| Figure 3.28 | Vehicle Translational Speed and Tyre Rotation Speed | 66 |
| Figure 3.29 | Vehicle Translational Speed and Tyre Rotation Speed | 67 |
| Figure4.1 | Area with maximum Misses stress | 71 |
| Figure 4.2 | Area with maximum Misses stress. | 71 |
| Figure 4.3 | Area with maximum pressure | 72 |
| Figure 4.4 | Deformation magnitude of tire after inflation | 73 |
| Figure 4.5 | Deformed direction of 2D axisymmetric half tire model after inflation | 74 |
| Figure 4.6 | Total time used to perform job for 2D axisymmetric half tyre model | 75 |
| Figure 4.7 | Total time for a complete 2D axisymmetric half tyre model analyses | 75 |
| Figure 4.8 | Area with maximum Misses stress | 76 |
| Figure 4.9 | Area with maximum principal stress | 76 |
| Figure 4.10 | Area with maximum pressure | 77 |
| Figure 4.11 | Magnitude of deformed full 2D axisymmetric tyre | 78 |
| Figure 4.12 | Magnitude of deformed full 2D axisymmetric tyre in U1 direction. | 78 |

| | | |
|-------------|--|----|
| Figure 4.13 | Magnitude of deformed full 2D axisymmetric tyre in U2 direction. | 79 |
| Figure 4.14 | Magnitude of deformed full 2D axisymmetric tyre in U3 direction. | 79 |
| Figure 4.15 | Magnitude of deformed full 2D axisymmetric tyre | 80 |
| Figure 4.16 | Total time used to perform job for 2D axisymmetric full tyre model | 80 |
| Figure 4.17 | Total time for a complete 2D axisymmetric full tyre model analyses | 81 |
| Figure 5.1 | Overview of free-free modal analysis | 85 |
| Figure 5.3 | Result of tyre free-free modal analysis of (1,0) mode: Mode shape and natural frequency | 88 |
| Figure 6.1 | Initial contact of road surface with tread surface | 92 |
| Figure 6.2 | Deformation of partial 3D tyre model after footprint analysis displacement control step | 92 |
| Figure 6.3 | Deformation magnitude of partial 3D tyre after footprint analysis with a loading of 1650N. | 93 |
| Figure 6.4 | Deformation direction and location of Partial 3D Tyre Footprint Analysis | 94 |
| Figure 6.5 | Stress distribution of tyre reinforced cord, belt member 1 | 95 |
| Figure 6.6 | Stress distribution of tyre reinforced cord, belt member 2 | 95 |
| Figure 6.7 | Stress distribution of tyre reinforced cord, carcass | 96 |
| Figure 6.8 | Stress distribution of tyre rubber matrix | 97 |
| Figure 6.9 | Shearing stress distribution of tyre in 1,2 plane | 98 |

| | | |
|-------------|---|-----|
| Figure 6.10 | Shearing stress distribution of tyre in 1,3 plane | 98 |
| Figure 6.11 | Shearing stress distribution of tyre in 2,3 plane | 98 |
| Figure 6.12 | Partial 3D tyre footprint contact nodal area | 99 |
| Figure 6.13 | Partial 3D tyre footprint contact normal force | 99 |
| Figure 6.14 | Partial 3D tyre footprint contact pressure | 99 |
| Figure 7.1 | Deformation contour of full 3D tyre model | 107 |
| Figure 7.2 | Deformation direction and location of Full 3D Tyre Footprint Analysis | 108 |
| Figure 7.3 | Stress distribution of tyre reinforced cord, belt member 1 | 109 |
| Figure 7.4 | Stress distribution of tyre reinforced cord, belt member 2 | 110 |
| Figure 7.5 | Stress distribution of tyre reinforced cord, carcass | 110 |
| Figure 7.6 | Full 3D tyre footprint contact nodal area | 111 |
| Figure 7.7 | Full 3D tyre footprint contact normal force | 112 |
| Figure 7.8 | Full 3D tyre footprint contact pressure | 112 |
| Figure 8.1 | Definition of tyre entering and leaving curvature | 116 |
| Figure 8.2 | Tyre contact path pressure distribution and shifting during steady state rolling analysis, full braking condition. | 118 |
| Figure 8.3 | Tyre contact path pressure distribution and shifting during steady state rolling analysis, full traction condition. | 119 |

| | | |
|-------------|---|-----|
| Figure 8.4 | Tyre contact shear stress distribution during steady state rolling analysis, full braking condition | 120 |
| Figure 8.5 | Tyre contact shear stress distribution during steady state rolling analysis, full traction condition | 121 |
| Figure 8.6 | Deformation of Tyre in longitudinal direction during steady state rolling analysis, full braking condition | 123 |
| Figure 8.7 | Deformation of Tyre in longitudinal direction during steady state rolling analysis, full traction condition | 125 |
| Figure 8.8 | Stress distribution of tyre belts member 1 during steady state rolling analysis, full braking condition | 127 |
| Figure 8.9 | Stress distribution on steel belt member 1 during full traction | 128 |
| Figure 8.10 | Stress distribution of tyre belts member 2 during steady state rolling analysis, full braking condition | 129 |
| Figure 8.11 | Stress distribution on steel belt member 1 during full traction | 130 |
| Figure 8.12 | Stress distribution in tyre carcass during rolling | 131 |
| Figure 8.13 | Stress distribution in tyre during rolling | 131 |

LIST OF ABBREVIATIONS

| | | |
|--------|---|--|
| 2-D | - | Two- dimensional |
| 3-D | - | Three-dimensional |
| axi | - | axisymmetric |
| BEM | - | Boundary element Method |
| CAD | - | Computer aided design |
| CAE | - | Computer aided engineering |
| CGAX3H | - | Continuum axisymmetric triangular hybrid element with twist |
| CGAX4H | - | Continuum axisymmetric tetrahedral hybrid element with twist |
| FE | - | Finite element |
| FEA | - | Finite element analysis |
| kPa | - | Kilo Pascal |
| SMG | - | Symmetric model generation |
| SRT | - | Symmetric result transfer |